Dependence of magnetic penetration depth on the thickness of superconducting Nb thin films

A. I. Gubin,[1,2] K. S. Il'in,[3] S. A. Vitusevich,[1,*] M. Siegel,[3] and N. Klein[1]

[1]*Institut für Schichten und Grenzflächen and CNI—Centre of Nanoelectronic Systems for Information Technology, Forschungszentrum Jülich, D-52425 Jülich, Germany*

[2]*Usikov Institute for Radiophysics and Electronics, National Academy of Sciences of Ukraine, 61085 Kharkiv, Ukraine*

[3]*Institut für Mikro- und Nanoelektoronische Systeme, Universität Karlsruhe, D-76187 Karlsruhe, Germany*

(Received 10 January 2005; revised manuscript received 22 March 2005; published 3 August 2005)

In this paper we present the results of a systematic study on the magnetic field penetration depth of superconducting niobium thin films. The films of thicknesses ranging from 8 to 300 nm were deposited on a Si substrate by dc magnetron sputtering. The values of the penetration depth $\lambda(0)$ were obtained from the measurements of the effective microwave surface impedance by employing a sapphire resonator technique. Additionally, for the films of thickness smaller than 20 nm, the absolute values of $\lambda(0)$ were determined by a microwave transmission method. We found that the reduction of the film thickness below 50 nm leads to a significant increase of the magnetic field penetration depth from about 80 nm for 300 nm thick film up to 230 nm for a 8 nm thick film. The dependence of the penetration depth on film thickness is described well by taking into account the experimental dependences of the critical temperature and residual resistivity on the thickness of the niobium films. Structural disordering of the films and suppression of superconductivity due to the proximity effect are considered as mechanisms responsible for the increase of the penetration depth in ultrathin films.

DOI: 10.1103/PhysRevB.72.064503 PACS number(s): 74.25.Ha, 74.25.Nf, 74.45.+c

I. INTRODUCTION

Over a long period of time, the physics of thin films of normal metals and superconductors has attracted great attention since their unique properties and wide range of applications require devices made from ultrathin films. Thin films are usually dirtier than thicker films and especially than bulk material, that is to say, they contain a larger amount of defects of the crystalline structure. It has been predicted theoretically and demonstrated experimentally that electron-electron[1] and electron-phonon interactions[2] in dirty metals differ strongly from those for pure and bulk materials. For example, this results in a violation of Matthiessen's rule in thin films of normal metals and superconductors at temperatures above the critical temperature.[3] However, different superconducting materials exhibit different reactions to disorder. The reduction of a film thickness may result in an increase of the superconducting critical temperature (T_C) of such materials as aluminum and tin, while other superconductors like Pb, Bi, Nb exhibit opposite T_C dependence on thickness.[4,5]

With respect to thin films, it is very important to note that their properties and the performance of devices made from them are extremely sensitive to fabrication conditions. Small variations of a technological process might result in considerable changes in the properties of nearly identical devices, even those made from the same superconducting film. The development of thin-film superconducting devices, successful optimization of their performances for a given application area, for a defined temperature range of operation, for a specified spectrum and power level of exciting radiation are only possible on the basis of a profound knowledge of the properties of the real material they are made of.

Today's advanced technology allows films a few nanometers thick to be fabricated and patterned into devices with an in-plane dimension of several tens of nanometers. This means that the size of these devices is about the same as or even smaller than the characteristic lengths of the bulk superconductor: the coherence length (ξ_0) and magnetic field penetration depth (λ_0). An analysis of a distribution of the supercurrent over a cross section of a superconducting strip,[6–8] formation and dynamics of the magnetic vortices,[9–11] and nonequilibrium processes in thin-film structures[12,13] is based on actual values of these two characteristic lengths. In thin films in the dirty limit $\xi_0 > l$ (l is the electron mean-free path) λ and ξ become dependent on l.[14] The theory predicts that the coherence length is proportional to a square root of the electron mean-free path, $\xi \propto l^{0.5}$, as opposed to the increase of the magnetic field penetration depth with decreasing: $l\lambda \propto l^{-0.5}$. Moreover, in thin films, the effective penetration depth (λ_{eff}) might even be much larger. If the film thickness (d) is much smaller than λ the effective penetration depth is proportional to d^{-1}.

Niobium superconducting thin films of thicknesses of about 10 nm or smaller are widely used for fabricating devices for different applications such as mixers[15] and detectors[16] of electromagnetic radiation. It is worth noting that at times these devices make conflicting demands on the film properties. For example, to reach the intermediate frequency bandwidth larger than 10 GHz the diffusion-cooled hot-electron bolometer mixer has to be made of Nb film with a large value of the electron mean-free path.[17] In contrast, the performance of the single-photon detector will be better for devices made from "dirty" superconducting films with small l.[18] Moreover, the difference between these two types of receivers determines the operation conditions of the superconducting film. In the case of the hot-electron bolometer mixer, the superconducting film is in the resistive state, and bias current is distributed uniformly over the cross section of the

film as in the normal state. In the superconducting single-photon detector, the film is kept in the superconducting state and biased by a current slightly below the critical value at operating temperature. In the latter situation, the distribution of the current over the cross section of a strip determined by the value of the magnetic field penetration depth has to be taken into account for the analysis of device performance.

The value of the magnetic field penetration depth $\lambda_0 = 47$ nm was obtained by Maxfield and McLean for a bulk Nb sample.[19] Larger values of λ of about 70–100 nm have been measured on Nb films of different thicknesses from 100 nm[20] up to a few micrometers.[21] Hsu and Kapitulnik[22] obtained $\lambda = 160$ nm on 2 nm thick single-crystal Nb film. Later, using the two-coil technique, Wang *et al.*[23] demonstrated a similar value (166 nm) of the penetration depth for 20 nm thick Nb film and smaller $\lambda \approx 95$ nm for a thicker (90 nm) film. The spread of the values of the magnetic field penetration depth reported in Refs. 19–23 is most likely determined by material properties rather than by the dimensionality of a film. Generally, one can draw only a qualitative conclusion that thinner films are characterized by a larger value of λ.

In the current paper, we present a systematic study of the magnetic field penetration depth in niobium thin films of thicknesses ranging from 8 nm ($\approx\lambda_0/6$) to 300 nm ($\approx 6\lambda_0$). The values of the penetration depth at zero temperature, $\lambda(0)$, were obtained by resonance and transmission microwave techniques. The experimental results concerning the $\lambda(0)$ dependence on film thickness are analyzed by using data on the critical temperature and residual resistivity obtained on the same Nb films. The paper is organized in the following manner. We briefly describe the technology of Nb thin film fabrication in Sec. II. The details of experimental methods for the determination of the magnetic field penetration depth in superconductors are presented in Sec. III. Experimental results will be discussed in Sec. IV. Section V is the conclusion.

II. FABRICATION AND CHARACTERIZATION OF Nb THIN FILMS

We deposited niobium films on $10.0 \times 10.0 \times 0.3$ mm silicon (100) substrates kept at room temperature by dc magnetron sputtering of a Nb target in argon atmosphere. The base pressure was about 10^{-6} mbar. The thickness d of the Nb films was inferred from the sputtering time after accurate calibration of the deposition rate (≈ 2 nm/s). Nb films of thicknesses from 8 to 300 nm were deposited. The temperature dependences of the resistance $R(T)$ of as-deposited Nb films were measured by a standard four-probe method. The width of the resistive transition was typically less than 0.1 K, even for the thinnest films. The superconducting critical temperature T_C was determined as the midpoint between the temperatures of the 10% and 90% normal resistance R_N at $T > T_C$ on the residual resistance plateau of $R(T)$. The value of the normal state residual resistivity (ρ_0) was obtained from R_N and the known geometrical dimensions of the sample. The dependences of T_C and ρ_0 on the thickness of the Nb films are shown in Fig. 1. It can be seen that T_C (circles in Fig. 1) gradually decreases with a reduction of the thickness from 300 to about 50 nm. A much stronger dependence of the critical temperature on thickness is observed for films thinner than 50 nm. We have to note that the critical temperature of the thickest 300 nm thick Nb film is about 9.7 K. This value is about half a Kelvin higher than the T_C usually reported for bulk Nb. The possible reasons for this result will be briefly discussed in Sec. IV A. The reduction of T_C with decreasing thickness is accompanied by increasing residual resistivity, shown in Fig. 1 by triangles.

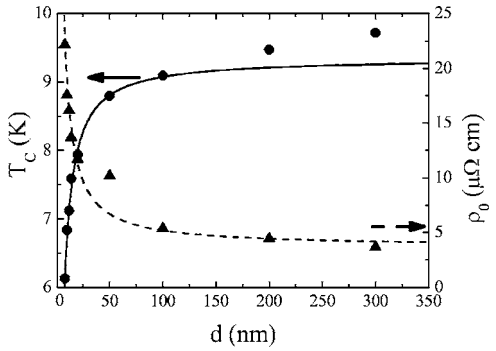

FIG. 1. The thickness dependence of the critical temperature (circles) and the residual resistivity in the normal state (triangles) of the Nb films. The solid line is the fit of $T_C(d)$ by Eq. (11) and the dashed line is the approximation of $\rho_0(d)$ by Eq. (12).

III. METHODS FOR PENETRATION DEPTH DETERMINATION

We used two different microwave methods to obtain the value of the magnetic field penetration depth $\lambda(0)$ in the Nb thin films.

A. Resonance method

The first method[24,25] is based on temperature variations of the resonance frequency of the sapphire dielectric resonator shielded by a copper cavity, in which one part of the endplate is replaced by the sample (superconducting film) under investigation. The temperature change of the penetration depth of superconducting film results in changes of the resonance frequency f_C of the sapphire dielectric resonator. A shift of $f_C(T)$ with respect to the resonance frequency measured at a reference temperature T_{ref} gives the variation of the effective penetration depth ($\delta\lambda_{eff}$) of the film-substrate structure[25] according to

$$\delta\lambda_{eff}(T) = \lambda_{eff}(T) - \lambda_{eff}(T_{ref}) = -\frac{G}{\pi\mu_0}\frac{f_C(T) - f_C(T_{ref})}{f_C^2(T_{ref})}, \tag{1}$$

where G is the geometrical factor of the sample inside the cavity and μ_0 is the dielectric permeability of the vacuum. The reference temperature is chosen in the range of $T \ll T_C$, where $\delta\lambda_{eff}(T) \ll \lambda_{eff}(0)$. The effective penetration depth λ_{eff} is[25]

$$\lambda_{\text{eff}} = \lambda \coth\left(\frac{d}{\lambda}\right), \tag{2}$$

where λ is the penetration depth of the superconductor. In the limit of infinite film thickness, where $d \gg \lambda$, the effective penetration depth is equal to λ. In the opposite limit ($d \ll \lambda$) λ_{eff} is much larger than λ: $\lambda_{eff} = \lambda^2/d$.

The value of the effective penetration depth and, consequently λ (2), can be obtained from a theoretical fit of the experimental dependence of $\delta\lambda_{eff}$ on temperature. The temperature dependence of the penetration depth $\lambda(T)$ of the superconducting film with nonmagnetic impurities can be written in the following form:[26]

$$\lambda(T) = \lambda(0)\left[1 - 2\int_{\Delta(T)}^{\infty} -\frac{\partial f(\varepsilon)}{\partial \varepsilon}\frac{\varepsilon\, d\varepsilon}{\sqrt{\varepsilon^2 - \Delta^2(T)}}\right]^{-1/2} \times \frac{\sqrt{1 + \frac{\xi_0}{J(T)l}}}{\sqrt{1 + \frac{\xi_0}{l}}},$$

$$\text{with} \quad f(\varepsilon) = \left[1 + e^{\varepsilon/k_B T}\right]^{-1}, \tag{3}$$

representing the Fermi function. In Eq. (3), $\Delta(T)$ is the temperature dependence of the superconducting energy gap[27] and the value of $J(T)$ changes smoothly from 1 at $T=0$ K to 1.33 at $T=T_C$.[26]

B. Transmission method

The value of the penetration depth can be also obtained from measurements of the temperature dependence of the microwave power transmitted through the film-substrate structure.[28–30] The film-substrate structure is placed between two waveguide sections in such a manner that electromagnetic radiation of frequency f is normally incident upon the film surface. The ratio of the transmitted to the incident power Tr is measured as a function of temperature. In the plane wave approximation the complex transmission coefficient Tr (Refs. 29 and 30) of the structure consisting of a film and dielectric substrate with thicknesses of d and d_S, respectively, is equal to

$$\text{Tr} = \frac{2n_f n_s}{2n_f n_s \cos\psi\cos\phi - (n_f^2 + n_s^2)\sin\psi\sin\phi - i(1+n_s^2)n_f\cos\phi\sin\psi - i(1+n_f^2)n_s\sin\phi\cos\psi}, \tag{4}$$

where $n_f = \sqrt{\varepsilon_f}$ and $n_s = \sqrt{\varepsilon_S}$ are the refractive indexes of the film and substrate, respectively, $\phi = k\, d n_f$, $\Psi = k\, d_S n_S$, $k = 2\pi/\lambda$. The dielectric function of the superconducting film, ε_f, is

$$\varepsilon_f = 1 + \frac{\sigma_N}{i\omega\varepsilon_0} - \frac{1}{\omega^2\varepsilon_0\mu_0\lambda^2}, \tag{5}$$

where σ_N is the normal state conductivity, $\omega = 2\pi f$, and ε_0 is the dielectric permittivity of the vacuum.[31]

The absolute value of the penetration depth is obtained from (5) using σ_N of the film estimated from the surface resistance R_S of the film.[26] The temperature dependence of the microwave surface resistance can be determined using the sapphire dielectric resonator technique described in Sec. III A. In the course of the measurements, the unloaded quality factor Q_0 of the dielectric resonator is recorded as a function of temperature. The effective surface resistance of the film-substrate structure is determined according to

$$R_S^{eff} = G\left(\frac{1}{Q_0} - \frac{1}{Q_{ref}}\right), \tag{6}$$

where Q_{ref} is the unloaded quality factor of the reference sample with R_S approaching zero. The microwave surface resistance R_S of the film of thickness d is determined from the impedance transformation:[25]

$$R_S^{eff} = R_S\left(\coth(d/\lambda) + \frac{d/\lambda}{\sinh^2(d/\lambda)}\right) + n_s\frac{(\omega\mu_0\lambda)^2}{Z_0}\frac{1}{\sinh^2(d/\lambda)}, \tag{7}$$

where $Z_0 = 377\ \Omega$ is the impedance of the free space.[25] The value of the penetration depth at zero temperature $\lambda(0)$ is obtained by extrapolation of experimental data on $\lambda(T)$ to $T=0$ K (the accuracy of this extrapolation is high enough because changes of the penetration depth at low temperatures are very small).

The two methods of determining the magnetic penetration depth of thin superconducting films described above complement each other. The transmission method is applicable for very thin films ($d < 0.5\lambda$) only. The microwave signal transmitted through thicker films is too weak to be measured. At the same time, the microwave resonator technique described in Sec. III A is suitable for relatively thick films. Using this technique, it is impossible to measure a large value of the effective penetration depth (tens of microns) at temperatures close to T_C for Nb films thinner than 50 nm with high accuracy. Films of this thickness are almost transparent in the microwave range at these temperatures and the resonance peak has an amplitude close to the noise level. Thus, only using both methods are we able to determine the penetration depth with sufficiently high accuracy in the whole range of film thickness of interest to us: from a few nanometers up to half a micron.

IV. RESULTS AND DISCUSSION

A. Critical temperature and residual resistivity

According to Eq. (3), the value of the penetration depth depends on the ratio of the Bardeen-Cooper-Schriffer (BCS) coherence length ξ_0 and electron mean-free path l. In the BCS theory the coherence length is

$$\xi_0 = \frac{\nu_F}{\pi\Delta}, \tag{8}$$

where ν_F is the Fermi velocity and $\Delta = A k_B T_C$ is the superconducting energy gap ($A = 1.765$ for weakly coupled superconductors). The electron mean-free path is inversely proportional to residual resistivity in accordance with the Einstein relation:

$$l = \frac{3}{e^2 N(0) v_F \rho_0}, \tag{9}$$

where e is the electron charge and $N(0)$ is the density of the electron state at the Fermi level. Finally, we obtain

$$\frac{\xi_0}{l} = \frac{\nu_F^2 e^2 N(0)}{3\pi A k_B} \frac{\rho_0}{T_C}. \tag{10}$$

Thus the ratio of ξ_0/l is proportional to the ratio ρ_0/T_C.

A decrease of the transition temperature in ultrathin superconducting films similar to that presented in Fig. 1 has been reported previously by many authors.[32,33] The interpretation of these results is based on several approaches,[4,34,35] of which the proximity effect is the one most frequently used.[36–38] In this model, the superconducting interaction is destroyed within the surface and film-substrate interface layers of thickness Δd on both sides of the film. These two layers have a much lower critical temperature in comparison with the rest of the film. Usually, in Nb films the formation of the niobium mono-oxide with a critical temperature of about 1.4 K is considered.[39] To verify this model we studied our Nb films using the secondary ion mass spectroscopy (SIMS) technique. For the SIMS measurements, a special layered 600 nm thick Nb film structure was deposited. At first, 400 nm of Nb was deposited on the silicon substrate. After deposition, the film was exposed to normal air for 24 hours and after that another 200 nm of Nb was deposited on top of the first layer. Results of this study (see Fig. 2) confirm the presence of oxygen on the surface and film-substrate interface layers. In contrast to previous studies, we found carbon in the same layers. We assume that carbon acts as an impurity and destroys superconductivity in these layers completely. In this situation, we consider the superconducting film as a normal-metal-superconductor-normal-metal (NSN) structure. Due to the proximity effect between these two nonsuperconducting layers and the central superconducting part of the film the superconductivity is suppressed and the critical temperature of the films becomes lower than that of the bulk sample.

This approach was first applied to thin superconducting films by Cooper.[36] He predicted that the critical temperature can be written in the following form:

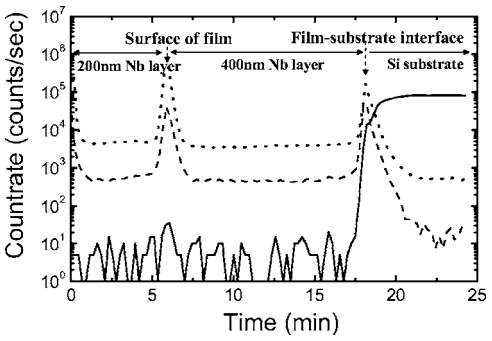

FIG. 2. The result of the SIMS study of the Nb film. The solid, dashed, and dotted lines are ion responses of silicon (substrate), carbon, and oxygen, respectively. The areas A and B correspond to 200 and 400 nm thick Nb layers, respectively. Area C corresponds to the Si substrate. Peak 1 of the oxygen and carbon responses is the position of the surface layer of the 400 nm Nb film. Peak 2 is the position of the film-substrate interface layer.

$$T_C(d) = T_C(\infty)\exp\left(\frac{l - 2\,\Delta d}{NV(d - 2\,\Delta d)}\right), \tag{11}$$

where $T_C(d)$ is the critical temperature of the film of thickness d, $T_C(\infty)$ is the critical temperature of an infinitely thick film, NV is the bulk interaction potential (0.32, for Nb[40]), and Δd is the thickness of a layer with destroyed superconductivity. From the best fit of experimental data by Eq. (11) (the solid line in Fig. 1), we obtained $T_C(\infty)$ of about 9.35 K, which is quite close to the critical temperature value for bulk Nb samples. The thickness Δd was determined as 0.5 nm from the same fit. It can be seen in Fig. 1 that Eq. (11) fits our experimental results for films of thicknesses in the range from 8 to about 100 nm. Two experimental points related to the thickest films (200 and 300 nm) deviate from the fitting curve appreciably: the critical temperature of the 300 nm thick film is about 9.7 K. The reason for this deviation of T_C is not clear. It should be noted that in several publications, softening of the phonon spectrum in superconducting films was considered[41,42] as a possible reason for increasing T_C. The value of $T_C = 22$ K was predicted for Nb by Strongin *et al.*[42] An experimental observation of an increase of the critical temperature of Nb above 9.3 K was reported in Refs. 41 and 21. It seems that the phonon spectrum in our Nb films thicker than 100 nm differs from the spectrum in thinner films. A possible reason for the phonon spectrum modification might be different conditions for growing films of different thicknesses, resulting in internal stress or strain in thick films.[43,44] At the initial stage of film growth, Nb is deposited directly on a silicon substrate kept at room temperature. The structure and quality of the substrate surface significantly determine the structure of ultrathin films in this situation. With increasing sputtering time for the deposition of thicker films, we obtain films with a crystalline structure that is more and more independent of substrate properties. Additionally, the temperature of the film-substrate structure rises during deposition due to the transformation of the kinetic energy of Nb atoms into heat. This effect might also

influence the structure of the film and consequently the superconducting properties of the film.

The decrease of the critical temperature is accompanied by an increase of the residual resistivity ρ_0 (triangles in Fig. 1). The dashed line in Fig. 1 is an approximation of the experimental dependence of ρ_0 on thickness of the Nb film described by the following equation:

$$\rho_0(d) = \rho_0(\infty) + \frac{150}{d}, \tag{12}$$

where $\rho_0(d)$ (in $\mu\Omega$ cm) is the resistivity of a film of thickness d (in nm), and $\rho_0(\infty)=3.7$ $\mu\Omega$ cm is the residual resistivity of the infinitely thick Nb film.

The dependences of the critical temperature (11) and residual resistivity (12) on thickness of the Nb films thus obtained will be used further for an analysis of the results of the magnetic field penetration depth dependence on thickness in Sec. IV D.

B. Penetration depth: Resonance technique

The sapphire dielectric resonator shielded by a copper cavity with part of one endplate replaced by the sample was excited in the $TE_{01\delta}$ mode under weak coupling conditions at the resonance frequency $f_C \approx 18$ GHz. The changes of the resonance frequency of the dielectric resonator in the cavity with a Nb film were measured in the temperature range from 1.5 K up to the critical temperature of the film. Then the changes of the effective penetration depth $\delta\lambda_{eff}$ were calculated using Eq. (1). The geometrical factor of the cavity $G=730$ was estimated by numerical simulations[45] of the electromagnetic field distribution in the cavity.

In advance, we experimentally determined the temperature-dependent contributions to $\delta\lambda_{eff}$ caused by changes of the resonance frequency due to the thermal expansion of the material of the cavity walls and the temperature dependence of the skin depth in copper and the dielectric constant of sapphire. The unloaded quality factor and the resonance frequency were measured for the cavity with a Nb thin-film sample replaced by a copper plate of the same size. The experimental error of $\delta\lambda_{eff}$ determination caused by these factors was found to be less than 1 nm for the temperature range ($T=1.5-10.0$ K) of the measurements.

The dependences of $\delta\lambda_{eff}$ on temperature for the Nb films of three different thicknesses are shown in Fig. 3. The 200 nm thick film exhibits an usual increase in changes of the effective penetration depth at temperatures approaching T_C. At temperatures above the critical temperature there is saturation of $\delta\lambda_{eff}$ caused by small changes of the skin depth of Nb in the normal state. At temperatures lower than 4.5 K the changes of the penetration depth of the 200 nm film are smaller than the resolution of our experimental setup. This results in the second, low-temperature plateau in the $\delta\lambda_{eff}(T)$ dependence.

The curves corresponding to thinner (8 and 20 nm) films shift to lower temperatures as a consequence of the reduction of the critical temperature of the films already discussed in Sec. IV A. Simultaneously, $\delta\lambda_{eff}$ increases for thinner films with respect to thicker ones.

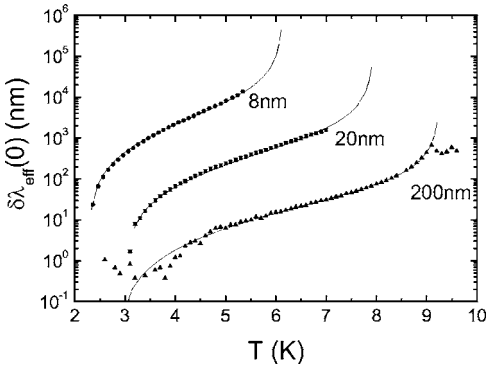

FIG. 3. The temperature dependence of changes in the effective penetration depth $\delta\lambda_{eff}$ of the Nb films with the different thicknesses indicated next to each curve. The solid lines are fitted by Eq. (1).

The value of the penetration depth at zero temperature $\lambda(0)$ was obtained from a fit of $\delta\lambda_{eff}(T)$ (solid lines in Fig. 3) using Eq. (3) with $\Delta(0)/k_BT_C=2$ and $\lambda(0)$ as the fit parameter. In accordance with Eq. (10), we estimated the value of the ratio ξ_0/l for all films studied taking $v_F=6\times10^7$ cm/s and using the material constant of Nb, $\rho_0 l=3.72\times10^{-6}$ $\mu\Omega\times\text{cm}^2$ (Ref. 46) for estimation of the electron mean-free path. The dependence of ξ_0/l on the Nb film thickness is shown in Fig. 4. It is seen that for films thinner than 50 nm we are able to perform calculations of the penetration depth in the dirty limit since $\xi_0/l>10$. For thicker films, the coherence length is about the value of the electron mean-free path and we made our calculations using the full expression, Eq. (3), for the temperature dependence of λ. The solid line in Fig. 4 is the dependence of the ξ_0/l ratio on film thickness simulated using the thickness dependences of the critical temperature, Eq. (11), and the residual resistance, Eq. (12). The dependence of the penetration depth obtained by our resonance technique on thickness is shown later in Fig. 6 by solid circles.

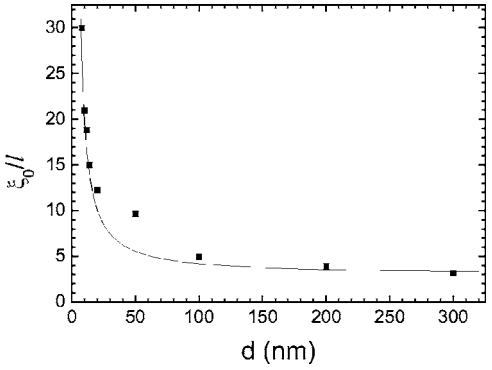

FIG. 4. The thickness dependence of the ratio between the coherence length ξ_0 and the electron mean-free path l of the Nb films determined from experimental data using Eq. (8) and Eq. (9), respectively. The solid line represents the simulation obtained by the substitution of $T_C(d)$ using Eq. (11) and of $\rho_0(d)$ using Eq. (12) into Eq. (10).

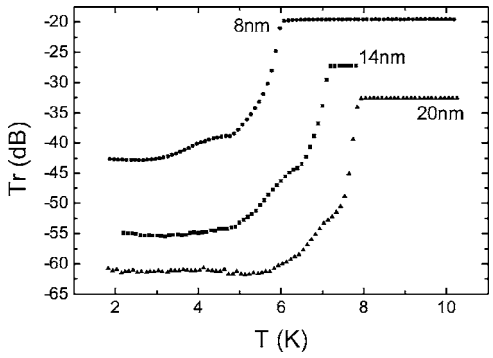

FIG. 5. The temperature dependence of the transmission coefficient Tr for three Nb films of different thicknesses d indicated next to each curve.

C. Penetration depth: Transmission technique

The values of the penetration depth were also evaluated from the temperature dependences of the ratio between the transmitted and incident power, using Tr, Eq. (4). The microwave power ($f=23.45$ GHz) transmitted through the Nb film-Si substrate structure arranged inside a waveguide was measured by a network analyzer. With our experimental setup based on an HP8722C network analyzer, we were able to measure the transmitted signal through Nb films thinner than 20 nm with high accuracy. The dielectric permittivity of the silicon substrate ($\varepsilon_S=12.1$ at $T=4.2$ K) required for the penetration depth determination by Eq. (4) was taken from the literature.[47] The imaginary part of the dielectric permittivity was obtained from measurements of the transmission coefficient through an uncoated silicon substrate.

The dependences of Tr on temperature for three different thicknesses of Nb films are shown in Fig. 5. Again we observe a shift of the experimental curves similar to the ones shown in Fig. 4 as a consequence of the reduction of the critical temperature with decreasing thickness. The nonmonotonic dependence of Tr at moderate temperatures is caused by nonmonotonic temperature growth during measurements and nonlinear temperature characteristics of the readout path and partially by standing waves inside the cryostat. However, the accuracy of the data obtained at the lowest temperature of the measurements is high enough due to the possibility of keeping this temperature stable for a long time.

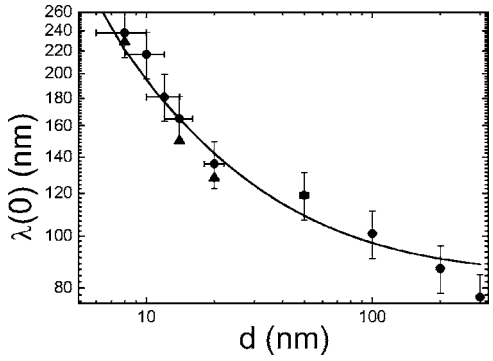

FIG. 6. The thickness dependence of penetration depth at zero temperature $\lambda(0)$. The circles represent results of resonance technique measurements, and the triangles are results of transmission measurements. The solid line represents the simulation of $\lambda(0)$ by Eq. (13) using $T_C(d)$ (11) and $\rho_0(d)$ (12).

There are two plateaus in the temperature dependences of the transmission coefficient. The saturation of Tr at low temperatures is determined by small changes of the penetration depth at $T<0.5T_C$ (3). At temperatures above the critical temperature, the films are in the normal state and the transmission coefficient is almost constant due to the very weak dependence of conductivity of the Nb film at temperatures much lower than the Debye temperature. The absolute value of the transmission coefficient, both for the normal and superconducting state, decreases with increasing thickness and reaches values of lower than −60 dB for the 20 nm thick film in the superconducting state.

The values of the magnetic penetration depth obtained from transmission measurements are shown in Fig. 6 by triangles. It can be seen that the values of the penetration depth obtained by both resonance and transmission techniques are in good agreement.

D. Penetration depth: Dependence on thickness

The experimental dependence of $\lambda(0)$ on the thickness of the Nb films is shown in Fig. 6. It is seen that $\lambda(0)$ increases gradually with the reduction of thickness from 300 down to about 50 nm and sharply for thickness smaller than 20 nm, and reaches a value of about 230 nm for the 8 nm thick Nb film. The BCS theory predicts the following value of the penetration depth at zero temperature:[26]

$$\lambda(0)=\lambda_L(0)\sqrt{1+\frac{\xi_0}{l}}, \tag{13}$$

where $\lambda_L(0)$ is the London penetration depth at $T=0$ K. Taking Eq. (10) into account and using the dependences of T_C and ρ_0 on thickness given by Eq. (11) and Eq. (12), respectively, we obtain the dependence of the penetration depth on the thickness of the Nb film. As a result of the analysis of the $\lambda(d)$ data shown in Fig. 6, $\lambda_L(0)$ was determined as 43 nm. This value of $\lambda_L(0)$ is close to previously reported results for bulk Nb.[19]

It can be seen that the experimental results are in good agreement with simulations based on Eq. (13) for films of thicknesses in the range from 8 to 200 nm. The experimental point corresponding to the 300 nm thick film deviates from (13) significantly. As we already mentioned earlier in this section, the value of the critical temperature of this film is about 9.7 K and is much higher than the fit (11) of the dependence of T_C on film thickness (see Fig. 1).

Considering the dependence of $\lambda(0)$ on thickness, we distinguish two mechanisms responsible for the increase of the penetration depth with decreasing thickness. The critical temperature and, corresponding to (8), the coherence length ξ_0 of the thin Nb films (at least for the films thinner than 100 nm), is determined by the proximity effect described by (11). Thus, the presence of the layers with destroyed superconductivity is the first reason for the modification of the penetration depth. The second one is strengthening of the

film disordering accompanying reduction of the film thickness. Quantitatively, this mechanism is described by the dependence of the residual resistivity of Nb on film thickness (12).

In the framework of this model, there are different possibilities for adapting the value of the magnetic field penetration depth for a certain application. A variation in the technology of the Nb thin film can result in changes of λ. Applying additional efforts for the precleaning of a substrate surface before deposition can significantly reduce the effective thickness of the nonsuperconducting film-substrate interface layer. As a result, the reduction of the critical temperature due to the proximity effect will be smaller. Heating of the substrate before and during film deposition usually leads to improvement of crystalline properties of the Nb films, i.e., to an increase of the electron mean-free path. According to Eq. (13), these modifications of the technology of thin film fabrication can result in λ approaching the λ_L value and weaker dependence on film thickness. In contrast, the increase of the λ value can be realized by coercive oxidation of the deposited film to suppress superconducting interaction and by ion bombardment to reduce the electron mean-free path value.

V. CONCLUSION

We experimentally obtained the dependence of the magnetic field penetration depth at zero temperature, $\lambda(0)$, on thickness of the Nb films in the range of film thicknesses from 8 to 300 nm by the microwave resonance and transmission techniques. It is important that the $\lambda(0)$ values obtained using both techniques are in good agreement. We have shown that the dependence of the penetration depth on thickness is well described by the BCS theory, taking into account real dependences of the critical temperature and residual resistivity on film thickness. The value of the penetration depth varies from about 80 nm for the thick ($d=200-300$ nm) films to 230 nm for the thinnest ($d=8$ nm) Nb film. The obtained value of the London penetration depth of $\lambda_L(0)=43$ nm for ultrathin Nb films is in good agreement with the previously reported data for bulk Nb. The proximity effect between the nonsuperconducting surface and film-substrate interface layers and the superconducting part of the film together with the disordering of the films structure determine the increase of the penetration depth at zero temperature in Nb thin films.

ACKNOWLEDGMENTS

The authors would like to acknowledge the contribution of U. Zastrow for the SIMS studies and B. B. Jin for helpful discussions. One of the authors (A. I. G.) is grateful for support by INTAS (fellowship Grant No. YSF 2002-183).

*Electronic address: s.vitusevich@fz-juelich.de; Fax.: +49-2461-612470

[1] B. L. Altshuler, A. G. Aronov, and D. E. Khmelnitskii, J. Phys. C **15**, 7367 (1982).
[2] A. Schmid, Z. Phys. **259**, 421 (1973).
[3] M. Yu. Reiser and A. V. Sergeev, Zh. Eksp. Teor. Fiz. **92**, 224 (1987) [Sov. Phys. JETP **65**, 1291 (1987)]; N. G. Ptitsina, G. M. Chulkova, K. S. Il'in, A. V. Sergeev, F. S. Pochinkov, E. M. Gershenzon, and M. E. Gershenson, Phys. Rev. B **56**, 10089 (1997).
[4] M. Strongin, R. S. Thompson, O. F. Kammerer, and J. E. Crow, Phys. Rev. B **1**, 1078 (1971), and references therein.
[5] J. Romijn, T. M. Klapwijk, M. J. Renne, and J. E. Mooij, Phys. Rev. B **26**, 3648 (1982).
[6] E. Zeldov, J. R. Clem, M. McElfresh, and M. Darwin, Phys. Rev. B **49**, 9802 (1994).
[7] G. Stejic, A. Gurevich, E. Kadyrov, D. Christen, R. Joynt, and D. C. Larbalestier, Phys. Rev. B **49**, 1274 (1994).
[8] D. M. Sheen, S. M. Ali, D. E. Oates, R. S. Withers, and J. A. Kong, IEEE Trans. Appl. Supercond. **1**, 108 (1991).
[9] A. V. Pan, R. Hohne, and P. Esquinazi, Physica B **329–323**, 1377 (2003).
[10] K. K. Likharev, Rev. Mod. Phys. **51**, 101 (1979).
[11] G. Stan, S. B. Field, and J. M. Martinis, Phys. Rev. Lett. **92**, 097003 (2004).
[12] W. J. Skocpol, M. R. Beasley, and M. Tinkham, J. Low Temp. Phys. **16**, 145 (1974).
[13] A. G. Sivakov, A. M. Glukhov, A. N. Omelyanchouk, Y. Koval, P. Müller, and A. V. Ustinov, Phys. Rev. Lett. **91**, 267001 (2003).
[14] P. B. Miller, Phys. Rev. **113**, 1209 (1959).
[15] B. S. Karasik, M. C. Gaidis, W. R. McGrath, B. Bumble, and H. G. LeDuc, Appl. Phys. Lett. **71**, 1567 (1997).
[16] A. Semenov, A. Engel, H.-W. Hübers, K. Il'in, and M. Siegel, *SPIE's 47th Annual Meeting*, Hawaii, August, 2002; *Millimeter and Submillimeter Detectors for Astronomy*, Proceedings of SPIE 4855, edited by T. G. Phillips and J. Zmuidzinas (California Institute of Technology, Pasadena, 2003), p. 249.
[17] D. E. Prober, Appl. Phys. Lett. **62**, 2119 (1993).
[18] A. Semenov, A. Engel, K. Il'in, G. Gol'tsman, M. Siegel, and H.-W. Hübers, Eur. Phys. J.: Appl. Phys. **21**, 171 (2003).
[19] B. W. Maxfield and W. L. McLean, Phys. Rev. **139**, A1515 (1965).
[20] A. Gauzzi, J. Le Cochec, G. Lamura, B. J. Jönsson, V. A. Gasparov, F. R. Ladan, B. Placais, P. A. Probst, D. Pavuna, and J. Bok, Rev. Sci. Instrum. **71**, 2147 (2000).
[21] D. Bloess, C. Durand, E. Mahner, H. Nakai, W. Weingarten, P. Bosland, J. Mayer, and L. Van Loyen, IEEE Trans. Appl. Supercond. **7**, 1776 (1997).
[22] J. W. P. Hsu and A. Kapitulnik, Phys. Rev. B **45**, 4819 (1992).
[23] R. F. Wang, S. P. Zhao, G. H. Chen, and Q. S. Yang, Appl. Phys. Lett. **75**, 3865 (1999).
[24] N. Klein, U. Dähne, U. Poppe, N. Tellmann, K. Urban, S. Orbach, S. Hensen, G. Müller, and H. Piel, J. Supercond. **5**, 195 (1992); N. Klein, German Patent No. DE 42 04 369 C2, 25 August 1994; U.S. Patent No. 5,506,497, 9 April 1996.

[25] N. Klein, H. Chaloupka, G. Müller, S. Orbach, H. Piel, B. Rosa, L. Schultz, U. Klein, and M. Peiniger, J. Appl. Phys. **67**, 6940 (1990).
[26] M. Tinkham, *Introduction to Superconductivity* (McGraw-Hill, New York, 1996).
[27] B. Mühlschegel, Z. Phys. **155**, 313 (1959).
[28] K. B. Bhasin, J. D. Warner, F. A. Miranda, W. L. Gordon, and H. S. Newman, IEEE Trans. Magn. **27**, 1284 (1991).
[29] B. J. Feenstra, *Proefschrift* (University of Groningen, the Netherlands, 1997), p. 162.
[30] N. T. Cherpak, A. I. Gubin, and A. A. Lavrinovich, Telecommun. Radio Eng. (Engl. Transl.) **55**, 81 (2001).
[31] I. B. Vendik and O. G. Vendik, *Physical Foundation of Superconductivity* (Scladen, St. Petersburg, 1997).
[32] S. A. Wolf, J. J. Kennedy, and M. J. Nisenoff, J. Vac. Sci. Technol. **13**, 145 (1976); S. A. Wolf, F. J. Rachford, and M. Nisenoff, *ibid.* **15**, 386 (1978).
[33] S. I. Park and T. H. Geballe, Physica B **135**, 108 (1985).
[34] Y. Oreg and A. M. Finkel'stein, Phys. Rev. Lett. **83**, 191 (1999).
[35] J. M. Graybeal and M. R. Beasley, Phys. Rev. B **29**, R4167 (1984).
[36] L. N. Cooper, Phys. Rev. Lett. **6**, 689 (1961).
[37] Ya. V. Fominov and M. V. Feigel'man, Phys. Rev. B **63**, 094518 (2001).
[38] V. Z. Kresin, IEEE Trans. Magn. **21**, 514 (1985).
[39] M. Gershenzon and V. Koshelets, Zh. Tekh. Fiz. **50**, 572 (1980). [Sov. Phys. Tech. Phys. **25**, 343 (1980)].
[40] R. Meservey and B. B. Schwartz, in *Superconductivity*, edited by R. D. Parks (Marcel Dekker Inc., New York, 1969).
[41] W. L. McMillan, Phys. Rev. **167**, 331 (1968).
[42] M. Strongin, O. F. Kammerer, J. E. Crow, R. D. Parks, D. H. Douglass, and M. A. Jensen, Phys. Rev. Lett. **21**, 1320 (1968).
[43] R. V. Amos, P. E. Breyer, H. H. Huang, and A. W. Lichtenberger, IEEE Trans. Appl. Supercond. **5**, 2326 (1995).
[44] T. Imamura, T. Shiota, and S. Hasuo, IEEE Trans. Appl. Supercond. **2**, 1 (1992).
[45] Microwave Studio™.
[46] A. F. Mayadas, R. B. Laibowitz, and J. J. Cuomo, J. Appl. Phys. **43**, 1287 (1972).
[47] M. Berlotti, V. Bogdanov, A. Ferrari, A. Jascow, N. Nazorova, A. Pikhtin, and L. Schirone, J. Opt. Soc. Am. B **7**, 918 (1990).